Film Boiling of Nitrogen with Suction on an Electrically Heated Horizontal Porous Plate: Effect of Flow Control Element Porosity and Thickness

V. K. PAI and S. G. BANKOFF

Northwestern University, Evanston, Illinois

Previous experimental work on film boiling of liquid nitrogen with vapor suction on an electrically heated horizontal porous plate (*1*) has demonstrated the necessity for a porous flow control element in order to stabilize the flow of liquid towards the plate. This element consisted of a relatively thick (1.5 in.) porous ceramic block interposed on the liquid side of the heated surface. In the absence of this element excessive local temperature nonuniformities and pressure oscillations were observed. Apart from undesirable local transient effects it was found that a portion of the heating surface would invariably quench to the bulk liquid temperature, resulting in incomplete vaporization of the liquid and excessive thermal stresses on the heating element. The wicklike action of the flow control element eliminates this unstable condition. With this stabilized system Wayner and Bankoff (*1*) and Wayner (*2*) showed that within certain limits the heat flux and vapor rate could be independently varied, and that there was an increase in the heat transfer coefficient by a factor of as much as 2.5 over that in nonporous film boiling. An added advantage was the appreciable superheat of the effluent vapor.

For the application of this principle to compact heat transfer devices the characteristics of the flow control element would be important in determining optimum performance. In the present work therefore the effects of porosity, pore diameter, and thickness of the flow control element on the heat transfer rate and on the stability of operation are studied.

EXPERIMENTAL APPARATUS

It is thought that an important application of the present principle would be in vaporization of cryogenic liquids. Liquid nitrogen 99.9% pure was therefore selected for this study because of its low cost and safety in handling.

The experimental apparatus, except for minor changes, has been described in detail (1, 2) and hence will only be briefly sketched here. A cross-sectional view of the heat transfer cell used is shown in Figure 1. A sintered two-layer composite of Rigimesh J with a composite thickness of 0.01 in. comprised the porous heating element (A). Rigimesh J is a sintered type 316 stainless steel screen with a wire count of 165 × 1,400. This heating element was silver soldered to copper strip leads (B) 0.013 in. thick and was held between two asbestos gaskets (C) which were cut so that a 1.75 in. square was available as the heat transfer area. Two 0.5 in. thick transite flanges (D) were used to connect the 3-in. I.D. Pyrex exhaust pipe (E). Saureisen No. 31 cement was used as a sealing agent. A pool of nitrogen (H), 5.4 in. in depth, at atmospheric pressure was maintained above the heating element in a styrofoam container (F), joined to the transite with nonhardening No. 2 Permatex gasketing cement (I). In order to reduce edge heat losses a heater (G) was installed around the heat transfer area, consisting of a nichrome tape (1/16 in. × 0.0045 in.) cemented into the upper transite piece, with power controlled by a separate variac.

Figure 2 shows the dimensions of the heat transfer surface and the thermocouple locations. Thirteen 30-gauge chromel-alumel thermocouples were welded to the bottom of the porous plate by an electric-arc discharge. The thermocouple junctions were uniformly coated with Saureisen No. 31 cement to protect them from mechanical stresses and to insulate the leads. The calibration of the thermocouples over a range be-

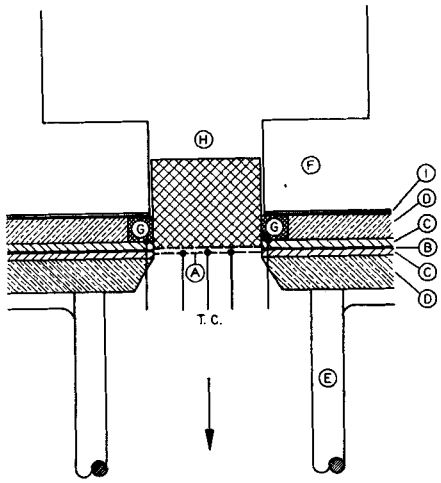

Fig. 1. Cross section of heat transfer cell.

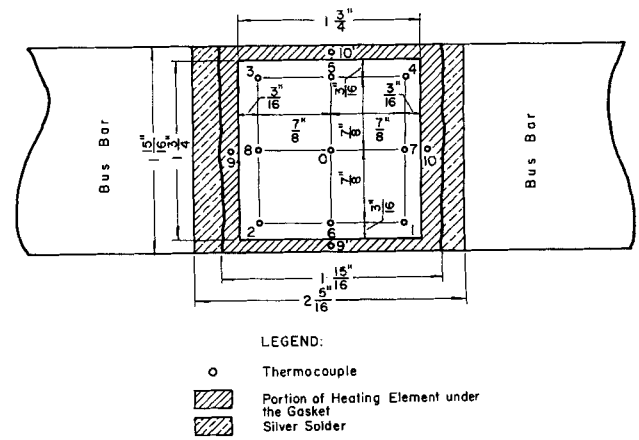

Fig. 2. Heat transfer surface.

tween the atmospheric boiling points of nitrogen and water was found to be in excellent agreement with published thermoelectric data. All the nonfluctuating thermocouple emfs were measured with a potentiometer with a stated limit of error of $\pm$ 0.05% + 3 μv.

The flow measurement system consisted of a calibrated rotameter and a vacuum pump. The pressure below the porous plate was measured with a manometer with a 0.827 sp. gr. liquid. Two chromel-alumel thermocouples, located 2 in. below the plate and shielded from radiation effects by a bed of 0.25-in. berl saddles, were used to measure the exhaust temperature.

The flow control elements used were glass-bonded quartz ceramic blocks of thickness L = 3/16, 1, and 1.5 in. Four different grades were employed as shown in Table 1.

These flow control elements were placed on the heating element with a 0.125-in. layer of 0.03-in. glass beads in between to insure uniform contact. In order to prevent the liquid nitrogen from bypassing the block it was sealed in place with cement, or with asbestos paper and cement, depending upon the thickness.

The power supply and control system consisted of a 5.75-kva. variac, a 3-kva. voltage stabilizing transformer, and a 15/1 step-down 20-kva. aircooled transformer. A vacuum tube voltmeter with an input impedance of 1 megohm was used to measure the voltage drop across the heating element. An instrument transformer with a ratio of 120/1 was used in conjunction with an a.c. ammeter to measure the current. The accuracy of the voltmeter was $\pm$ 1% and that of the ammeter $\pm$ 0.5% after calibration.

In order to make an accurate estimation of the surface temperature the heating element itself was used as a resistance thermometer. The electrical resistance of the heating element was measured during operation by an a.c. potentiometric technique given in reference *1*. A detailed description has not been previously published and hence is given here. The potential developed across the heating element is balanced against the potential developed across a known resistance in the secondary circuit of a current transformer, whose primary is in series with the resistance heater. The balance point is found as a minimum on an a.c. null detector. Figure 3 is an electrical diagram of the circuit used for measuring electrical resistance. The unknown resistance (R_x) was the resistance of the porous heating element. An a.c. null detector (N) with an input impedance of 10,000 Ω was used to determine the balance point. The current transformer (T), with a ratio of 120/1, was also used in the ammeter circuit. It was possible to switch the secondary of the transformer to either the ammeter or potentiometric circuit. A multitap resistor (R_3 = 13.500Ω), two constant resistors (R_1 = 31.510Ω and R_5 = 10.162Ω) and a slide wire resistor (R_4 = 0.4673Ω), all in series, were also connected across the secondary of the current transformer in parallel with a 2.496Ω resistor (R_2). The slide wire, which was 100 cm. long, was used to find the balance point within close limits, while the multitap resistor was used for larger increments of resistance. The resistance R_6 equal in magnitude to the input impedance of the null detector had no effect on the resistance calculations but increased the sensitivity of the null detector. From Figure 3, when the balance point is achieved, it follows that

$$R_x = \frac{R_p}{120\,(C+1)} \qquad (1)$$

where

$$C = \frac{R_1 + R_3 + R_4 + R_5}{R_2} \qquad (2)$$

TABLE 1. AVERAGE POROSITY AND PORE DIAMETER OF FLOW CONTROL ELEMENTS

Grade	ϵ, %	D_p, μ
Extra fine	26	55
Fine	29	110
Medium	34	150
Coarse	36	250

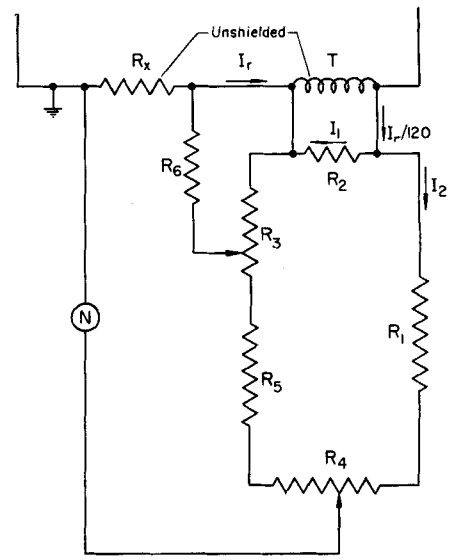

Fig. 3. A.C. potentiometric circuit. All elements shielded unless otherwise indicated.

The constantan measuring-circuit resistances were calibrated in place by Wayner (2) by d.c. potentiometric comparison with a standard resistance of 2.161Ω $\pm$ 0.05% using a millivolt potentiometer. In order to keep leakage currents and stray induced voltages to a minimum the measuring circuit was shielded as much as possible. The very small variation in the calibration correction factor demonstrated that the current transformer maintained a constant current ratio and that sufficient shielding was used to avoid induced errors. In addition to the individual resistance calibration it was necessary to check the overall a.c. potentiometric measuring technique against a known resistance at all power levels used during subsequent experimentation in order to determine if the power level had any effect on the resistance measuring circuit. To do this the regular stainless steel heating element was replaced by a constantan resistor 0.006069Ω $\pm$ 0.1% immersed in a constant temperature bath. The a.c. resistance as measured by the a.c. potentiometric circuit was 0.006161Ω $\pm$ 0.3% at a power level of 3.2 w. This gave an a.c. to d.c. calibration correction of 0.9867 for the potentiometric circuit at this power level. The difference between maximum and minimum calibration correction measured as a function of current was 0.25%, which was equal to 4°F. when a stainless steel heating element is used. This calibration correction was either a result of the slight phase shift between the secondary and primary of the current transformer, approximated at 1.5 deg. when an oscilloscope is used, or small induced currents.

The resistance of a stainless steel heating element of the type used in the present work was measured as a function of the temperature, by use of a small direct current, in comparison with a standard resistance of 2.161Ω $\pm$ 0.05%. The resistance and temperature were recorded at approximately 50°F. intervals from room temperature to 520°F. in an oven at the boiling point of liquid nitrogen and the freezing point of water and at a few intermediate points, with a refrigerator used. The resistance of the stainless steel heating element was measured at different times during its use with the a.c. potentiometric circuit at a power level of approximately 3.2 w. The average calibration correction was 0.9862, in excellent agreement with the calibration correction measured with the constantan resistor.

At high vapor flow rates through the porous plate the thermocouples were seriously in error because of their obstruction of the vapor flow. The arrangement of these thermocouples however made it possible to use them as resistance leads, thus giving the average temperature on different parts of the plate. The resistance of six different junctions (Figure 2, thermocouples 3-5, 8-0, 2-6, 6-1, 0-7, and 5-4) on the plate was calibrated as a function of temperature. During the operation these resistances were measured by the a.c. potentiometric circuit. This measurement is essentially unaffected by heat

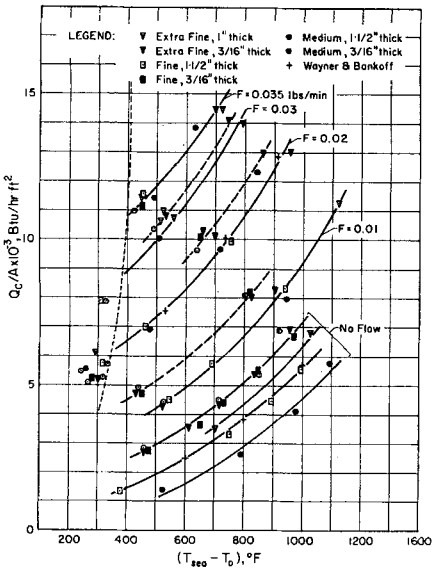

Fig. 4. Heat flux vs. temperature difference with flow rate as parameter for different flow control elements.

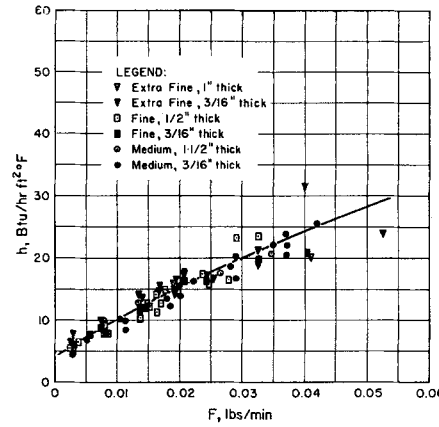

Fig. 5. Heat transfer coefficient vs. flow rate.

conduction losses in the resistance lead wires and thus gives a good estimate of temperature distribution.

OPERATION OF THE EQUIPMENT

All runs were made at approximately constant power input over a range of vapor flow rates from zero to the limiting flow rate at which a portion of the plate quenched to the liquid temperature. The power input to the guard heater around the heating element had to be controlled and kept at a low value so as to protect the styrofoam container and the cement seal. The result was an improved, but still nonuniform surface temperature distribution, as noted from the measurements of the resistances between various thermocouple junctions.

The surface temperature as read by the thermocouples and the a.c. potentiometric method showed no fluctuations at low flow rates. As the flow rate was increased, the signals from some thermocouples began to show slight fluctuations and eventually became large to be observed even on the a.c. null detector. The amplitude of these oscillations was maximum (>15°F.) just before the plate became partially quenched. A similar observation was made in (*1*). This confirms the strong possibility of liquid-solid contact, despite the fact that the film boiling regime prevailed.

When the coarse 1.5-in. block was used as a flow control element, it was not possible to sustain stable operation. Even at low vapor flow rates a part of the plate would slowly drift into nucleate boiling regime. No flow (and in some cases even flow reversal) of vapor would then occur in other portions of the plate, making them extremely hot. Violent agitation of the liquid could be observed, with vapor bubbles breaking away from the flow control element. The presumption therefore is that a stability plot in ϵ vs. D_p space would show a minimum porosity-pore diameter surface above which effective flow control is not possible.

CALCULATION AND ANALYSIS OF DATA

As in (*1*) the corrected heat flux was calculated by correcting the measured power input for conduction and radiation losses. Since the vapor exhausted through the heating element, convection was considered to be a part of the overall heat transfer mechanism. The magnitude of the correction for the heat losses was maximum (40 to 45% of the power input) at no flow and minimum (5 to 6% of the power input) at the limiting vapor flow rate.

In the calculation of the average surface temperature the method used in reference *1* was followed. The resistance of the heating element, measured during the operation by the a.c. potentiometric method, was corrected for the area of the heating element under the gasket with the temperatures read by the thermocouples under the gasket. The average surface temperature corresponding to this resistance was called T_{se}. This temperature was then converted into an area-average temperature T_{sea} from thermocouple data (*1*). This correction was usually very small (~3°F.).

The average heat transfer coefficient is now defined as

$$h = \frac{Q_c}{A(T_{sea} - T_o)} \tag{3}$$

The Nusselt number $Nu = hD_S/k_f$ is a function of the Reynolds number $Re = D_SG/\mu_f$, where the nitrogen thermal conductivity and viscosity are evaluated at the average of the saturated vapor and exhaust temperatures.

An error analysis of the data (3) indicates that the total relative error in the corrected heat flux is ± 5% due to errors in measurements of power input and in heat loss estimates. The maximum error in the average temperature difference $(T_{se} - T_o)$ is estimated to be ± 16°F., not including the effects of temperature distribution. The correction from T_{se} to T_{sea}, which includes the effects of temperature distribution, adds a possible error, depending on the flow and power conditions, of from 0 to 2.5% of the overall temperature driving force.

DISCUSSION OF RESULTS

In Figure 4 the heat flux Q_c/A is plotted as a function of area-average temperature difference $(T_{sea} - T_o)$, with vapor flow rate F as the parameter. The thin dotted envelope on the left is the limit of stable operation given in reference *1*. Data from (*1*) are also seen to agree very well with the present data. The points on the left of the envelope represent unstable points in the present work.

The effects of changes in the flow control element porosity and thickness are evident in Figure 4. There is a distinct effect on the heat transfer coefficient of the porosity and thickness of the block for the zero flow curves. Under these conditions the porous ceramic block acting as the flow controller also conducts an appreciable amount of heat away from the surface. As D_p decreases, the heat flux curve is displaced upwards, presumably on account of the higher thermal conductivity of the finer grades. For the thinner blocks (3/16 in.) the curve is displaced still

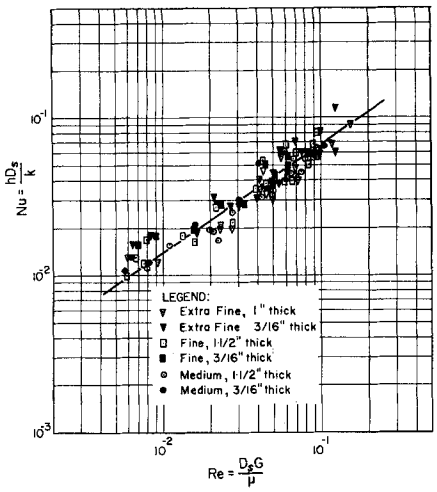

Fig. 6. Nusselt number vs. Reynolds number.

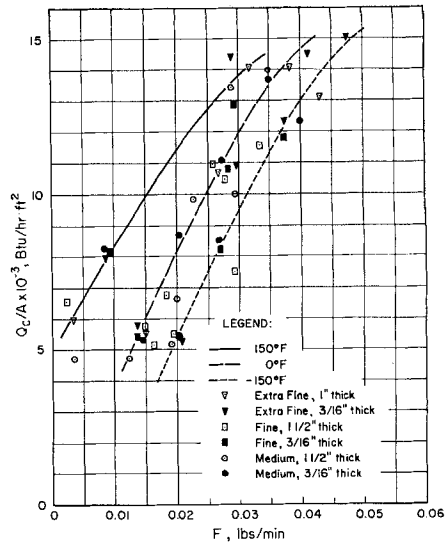

Fig. 7. Heat flux vs. rate for various exhaust temperatures.

further upwards because of the decreased thermal resistance of the fin. At this thickness the porosity effect is seen to be negligible at zero flow.

As the flow of vapor through the plate commences, the liquid comes closer to the surface and the heat transfer coefficient h increases, being principally determined by the flow rate. Once flow is established, the block porosity has little influence on the surface temperature. At low flow rates the surface temperature of the 3/16-in. block is less than that of thicker blocks, but as the flow rate is increased, this difference is reduced, and at a flow rate of about 1.40 lb. min.$^{-1}$ft.$^{-2}$ (F = 0.035 lb. min.$^{-1}$) the thin block behaves similarly to the thicker blocks.

It is of more interest however to note that the stability of the operation is not affected by the considerable reduction in L. Furthermore for L = 3/16 in. channeling of liquid or vapor through the block is greatly reduced, and the time required to attain steady state conditions is only half as much as for $L \geq 1$ in.

From Figure 5 it is clear that the heat transfer coefficient, defined by Equation (3), is principally a function of the flow rate. These data are replotted in Figure 6 to obtain the correlation equation

$$Nu = 0.402\ (Re)^{0.733} \qquad 0.007 < Re < 0.160 \qquad (4)$$

This is in excellent agreement with the relation given in (*1*) for a 1.5 in. thick fine grade block. Equation (4) indicates that the Nusselt number is a function of only the Reynolds number over the range of Re, L, and D_p tested and is independent of the nature of the flow control element, provided that stable operation is attainable.

In Figure 7 the heat flux is plotted as a function of the vapor flow rate with exhaust temperatures of 150°, 0°, and −150°F. as parameters. The curves indicate that the vapor is considerably superheated, in contrast to the vapor generated by normal film boiling. From these curves it can be seen that within the ranges of the variables studied the porosity and thickness of the flow control element have little effect on the temperature of the vapor.

The overall pressure drop through the system was of the order of 0.1 lb./sq.in. at the maximum flow rate used (1.65 lb. min.$^{-1}$ ft.$^{-2}$). There was a considerable scatter in the pressure drop data, attributed principally to changes in the permeability of the plate with temperature and time, as well as possible uneven flow distribution.

SUMMARY AND CONCLUSIONS

1. Film boiling of liquid nitrogen with vapor suction on a stainless steel porous plate with porous ceramic flow control elements of four different grades (range of average porosity 26 to 36%, range of average pore diameter 55 to 250μ) was studied in the superficial mass velocity range 0-1.65 lb. min.$^{-1}$ ft.$^{-2}$. Stable operation was not possible with the coarsest ceramic block, presumably because its flow resistance was too small.

2. The stability of operation was not affected by a reduction of thickness of the flow control element from 1.5 to 3/16 in. The thinner elements resulted in a lower surface temperature at low flow rates but performed similarly to the thicker blocks above a flow rate of about 1.40 lb. min.$^{-1}$ ft.$^{-2}$.

3. The exhaust vapor temperature ranged from as high as + 250° to — 320°F. depending on the flow rate and was largely independent of the nature of the flow control element.

4. Similarly the Nusselt number was a function of Reynolds number only for the flow control elements tested. It appears therefore that a considerable reduction in flow control element thickness may be anticipated. Agreement with previous work (*1*), wherein substantial improvement in the heat transfer coefficient over that of normal film boiling was reported, is excellent.

ACKNOWLEDGMENT

This work was supported by a grant from the National Science Foundation (G-20224). Mr. F. L. Maves assisted greatly in processing the experimental data.

NOTATION

A = area of heating element, sq.ft.
C = constant for the a.c. potentiometric circuit, Equation (2)
D_p = average pore diameter of the flow control element, μ
Ds = maximum diameter particle which will pass through the sintered screen, ft.
F = flow rate, lb./min.$^{-1}$
G = superficial mass velocity, lb./(hr.$^{-1}$) (ft.$^{-2}$)
h = average heat transfer coefficient, B.t.u./(hr.$^{-1}$) (ft.$^{-2}$/°F.$^{-1}$)
k_f = thermal conductivity of nitrogen, B.t.u./(hr.$^{-1}$) (ft.$^{-1}$/F.°$^{-1}$)
L = thickness of porous ceramic block, in.
Q_c/A = corrected heat flux, B.t.u./(hr.$^{-1}$/ft.$^{-2}$)
R = electrical resistance, Ω

R_x = measured resistance of the heating element, Ω
R_p = resistance between the two slide-wire contacts in the a.c. potentiometric circuit, Ω
T_o = temperature of saturated nitrogen at atm. pressure, °F.
T_{se} = average surface temperature, based on electrical resistance, °F.
T_{sea} = average surface temperature, based on electrical resistance, converted to area average, °F.
ϵ = average porosity of the flow control element, %
μ_f = viscosity of nitrogen, lb./(ft.$^{-1}$/hr.$^{-1}$)

LITERATURE CITED

1. Wayner, P. C., Jr., and S. G. Bankoff, *A.I.Ch.E. Journal*, **11**, No. 1, 59 (1965).
2. Wayner, P. C., Jr., Ph.D. thesis, Northwestern University, Evanston, Illinois (1963).
3. Pai, V. K., M.S. thesis, Northwestern University, Evanston, Illinois (1963).

Manuscript received August 7, 1963; revision received January 30, 1964; paper accepted January 30, 1964. Paper presented at A.I.Ch.E. Pittsburgh meeting.

Liquid Atomization in a High Intensity Sound Field

R. L. WILCOX and R. W. TATE

Delavan Manufacturing Company, West Des Moines, Iowa

High intensity sound was investigated as a means for liquid breakup. Sonic generators provided energy to atomize liquid introduced near the sound source. Droplet size was measured at several conditions of air and liquid flow for sound intensities ranging up to 160 decibels.

Atomization was good at low liquid flows but became rather coarse as flow rate increased. The droplet size distributions were not uniform. No improvement in breakup could be attributed directly to the sonic compressions and rarefactions beyond that normally produced by the tearing action of air in conventional two-fluid atomizers at comparable air/liquid ratios.

The purpose of this study was to determine if sound energy with its characteristic condensations and rarefactions could be made to disturb liquid sheets and streams and thereby improve atomization. One possible result would be nearly uniform droplets.

Rayleigh, Haenlein, and Weber observed uniform droplets from liquid jets (*1, 2*). A liquid jet becomes disturbed upon leaving the orifice. If this disturbance remains unchanged, a constant time lapse will occur from the beginning of the disturbance to formation of a drop. Therefore, the distance to droplet formation may be changed by varying the liquid velocity. Secondary dis-

TABLE 1. OPERATING CONDITIONS FOR HARTMANN ATOMIZER

	Figure 3 Droplet size distribution curve			
	A	*B*	*C*	*D*
Liquid feed	Annular sheet			
Sound frequency (kcycles)	42	18	*	42
Water flow (gal./hr.)	50			20
Water pressure (lb./sq. in.)	50			12
Air flow (lb./hr.)	15.4			
Air pressure (lb./sq. in.)	50			
Sauter mean diameter (μ)	158	139	124	21

* No resonant cavity.